JOURNAL OF MATERIALS SCIENCE 32 (1997) 5389–5403

Crystallization of glassforming melts under hydrostatic pressure and shear stress

Part I *Crystallization catalysis under hydrostatic pressure: possibilities and limitations*

I. GUTZOW
Institute of Physical Chemistry Bulgarian Academy of Sciences, Sofia 1113, Bulgaria
B. DURSCHANG, C. RÜSSEL
Otto-Schott-Institut für Glaschemie, Friedrich-Schiller-Universität, 07743 Jena, Germany

This is the first part of a thorough study of the kinetics of melt crystallization under applied static pressure, P, and under shear stress. The thermodynamic and kinetic consequences of increased external pressure on nucleation rate, non-steady-state time lag, rate of crystal growth and overall crystallization kinetics in undercooled melts are analysed. Two types of undercooled liquids (with either positive or negative volume dilatation upon crystallization) are considered. Particular attention is given to the effect of pressure on the specific interface energy, σ, at the crystal/melt phase boundary. Using an appropriate thermodynamic model it is shown that for one-component systems, $(\partial\sigma/\partial p) < 0$ is to be expected as a rule. Thus an additional decrease of the thermodynamic barrier of nucleation in pressurized melts is to be expected. However, it is also shown that the increase of melt viscosity with pressure in most cases reduces the effect of this decrease. Thus increased pressure has a limited effect as a nucleation catalyst. The possibilities in this respect are analysed and conditions under which static pressure may lead to enhanced crystallization are outlined.

1. Introduction

The influence of hydrostatic pressure on the processes of segregation and crystallization, especially in undercooled melts, has fascinated several generations of investigators. Beginning with Tammann [1] and his students [see 2, 3], the main emphasis was focused on any possible effect of pressure on the thermodynamically predicted rise of the melting point, T_m, of the substance when crystallization proceeds with positive dilatation, ΔV, (at $\Delta V > 0$). Thus the primary effect of pressure on crystallization of undercooled liquids was anticipated to result in an increase of the thermodynamic driving force of the process. The first quantitative estimate of this effect in terms of a decreased nucleation barrier, ΔW, was given, it seems, by Sirota [4]. A contemporary treatment of the thermodynamics of this problem may be followed in references [5–8]. The possibility of nucleation catalysis due to a sudden rise in pressure was also discussed in the above context by one of the classic authors of nucleation theory as far back as the early forties [8, 9].

Based on the present day general capillary model of nucleation theory it can be expected that the impact of pressure on the nucleation barrier, ΔW, could be more complex than initially suggested. According to a conjecture made by Uhlmann *et al.* [5] the possible change in specific free energy, σ, at the crystal/melt interface should also be accounted for in calculating, ΔW. However, Uhlmann *et al.* [5] proposed no model to introduce a corresponding correction. An attempt in this direction is made in the present contribution and this is the first objective of the paper.

Even in the first analyses of melt crystallization experiments performed under pressure [2, 3] it was anticipated that a kinetic factor, the increase in viscosity η of the melt under hydrostatic pressure, may reduce or even nullify the thermodynamically expected nucleation or crystal growth rate increase. More elaborate considerations in this respect can also be found in references [5, 6].

The elucidation of the influence of external pressure on viscosity and thus on crystallization and vitrification processes in glassforming melts is the second aim of our investigation. Both effects, on ΔW (via the melting point shift and by changing σ) and on η, are treated here in the framework of one and the same model. In this way the possibilities and limitations of increased pressure as a catalyst of crystallization in undercooled glassforming melts could be analysed in more general and quantitative terms. Such a more general treatment is the third aim of the present study.

The result of the analysis performed in the first part of the present contribution can be briefly summarized in the following way: only in exceptional cases (e.g., at

0022–2461

very high, non-typical ΔV values and at relatively high pressures – in the GPa region) can static pressure exert a real catalytic effect upon crystallization. In most cases of melt crystallization, no increase in nucleation rate, but rather a shift in nucleation rate as a function of temperature curves to higher temperatures is to be expected under pressure. As a rule, the crystal growth rate is not augmented but inhibited by external pressure.

There are however experiments indicating that even under relatively low pressures nucleation and crystal growth are readily initiated in typical glassforming melts, even in cases where minimal dilatation effects are to be expected upon crystallization. A closer examination shows that these are always cases where the melt is exposed to both hydrostatic pressure and tangential stress, i.e., these are cases of crystallization of undercooled melts flowing under pressure. Evidence in support of this conclusion was obtained (see [10, 11]) in the development of a new technologically promising process, namely the synthesis of glass–ceramic materials with an oriented structure by means of extrusion pressure techniques. Extrusion pressing of glassforming melts [12, 13] and of glass–ceramics [14] has been known for many years. We have shown [10, 11] that under the conditions of this process, crystallization (both nucleation and growth) is in fact catalysed.

The above evidence is also supported by the results of the remarkable experiments performed several years ago by Pennings *et al.* [15] using undercooled polymer melts. In these experiments flow of the undercooled melt under shear stress (with no hydrostatic pressure applied) initiated crystallization. In these experiments no reduction of the thermodynamic barrier, ΔW, could be expected. The only logical explanation of the catalytic effect on nucleation observed in this work is that shear flow reduces the viscosity of the melt and hence lowers the kinetic barrier of nucleation and crystal growth.

A shear flow induced decrease in melt viscosity is known to be inherent to the very nature of the pseudoplastic non-Newtonian flow behaviour of such liquids as organic polymers or silicate and other inorganic glassforming melts. To confirm the assumption of such a reduction of the kinetic barrier of crystallization we use the results obtained in our previous investigation on the non-Newtonian behaviour of glassforming liquids [16, 17].

The study of this new and promising field of hydrodynamically induced nucleation catalysis and its combination with processes of crystallization under static pressure is the main target of our research efforts in the second part of the present article. It shows that such a combination has significant technological perspectives and offers new possibilities in examining and predicting crystallization in a wide range of natural processes and technological applications.

We begin the analysis with the formalism of the thermodynamics of melt crystallization under hydrostatic pressure. There then follows an examination of the kinetic effects induced by pressure in the crystallization of undercooled liquids.

2. Thermodynamics of melt crystallization under hydrostatic pressure

Three problems have to be considered here:

2.1. Dependence of the melting point, T_m, on pressure

It follows directly from the Clausius–Clapeyron equation that:

$$d(T_m)/dP = \Delta V/\Delta S \quad (1)$$

In our case $\Delta V = V_{(f)}(T) - V_{(c)}(T)$ and $\Delta S = S_{(f)}(T) - S_{(c)}(T)$ denote the differences in the molar volumes and entropies of the liquid (f) and of the crystal (c). Integration of Equation 1 under the assumption $(\Delta V/\Delta S) \approx$ const. $= (\Delta V_m/\Delta S_m)$ leads to:

$$T_m(P) - T_m(O) \cong (\Delta V_m/\Delta S_m)(P - P_o) \quad (2)$$

where $T_m(P)$ denotes the melting point at increased pressure P and $T_m(O)$ stands for the melting point at normal (atmospheric) pressure P_o (usually $P \gg P_o$ and thus in most cases $(P - P_o) \approx P$). The above assumption implies that: (i) the two phases (f) and (c) are considered as incompressible, and (ii) in estimating $(\Delta V/\Delta S)$ the change in volume, ΔV_m, at the melting point T_m (for $T_m(O)$ and $P = P_o$) and the respective entropy of melting, ΔS_m, are accounted for. This assumption, as demonstrated in Fig. 1, usually leads to quite satisfactory results, when pressures below 1 GPa are involved. When ΔV_m or ΔS_m are not known, the volume and entropy difference, ΔV_g and ΔS_g, at the temperature of vitrification, T_g, (for $P = P_o$) can be used instead, for an estimation. These values ΔV (and ΔS_m) were in fact used in drawing the straight line given in Fig. 1.

In a previous paper (see [19] and in more detail [20]), we have shown that based on the simple lattice–hole models of the free volume theory of

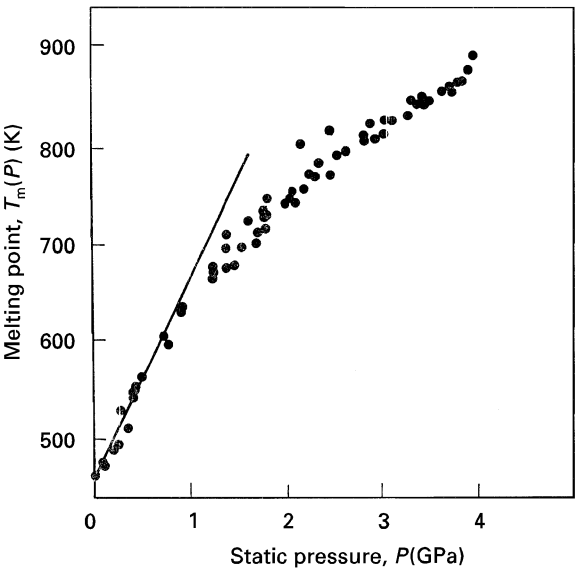

Figure 1 Shift of the melting point $T_m(P)$ of selenium under hydrostatic pressure. Straight line: according to Equation 2 with $\Delta V(g) = 2.06\ cm^3$ mol and $\Delta S_m = 10_p\ gJ$/grad mole. Black points: experimental data according to Klement *et al.* [18].

liquids (i.e., for $\Delta V > 0$) the following approximation can be derived for the two quantities appearing in Equation 1:

$$\Delta S \approx 3R(\Delta V/V_c) \tag{3}$$

Thus $(\Delta V/\Delta S) \approx$ const. $= V_c/3R$ (where R is the gas constant) can be expected to give a first approximation in Equation 2 in accordance with experimental findings.

A more accurate estimation for the course of the $T_m(P)$ function, applicable also at higher pressures, is discussed by Aziz *et al.* [6]. Here we shall use Equation 2 mostly in the form:

$$T_m(P) \cong T_m(O) f_1(P) \tag{4}$$

where

$$f_1(P) = \{1 + [\Delta V_m/\Delta S_m T_m(O)](P - P_o)\} \tag{5}$$

In the following derivations we introduce in a similar way several dimensionless pressure dependent functions, $f_i(P)$, introduced in such a way that $f_i(P_o) \equiv 1$. With the help of these functions a direct transformation of the thermodynamic and kinetic dependences derived for atmospheric pressure ($P = P_o$) into such corresponding to crystallization at increased pressure is easily performed.

2.2. Thermodynamic driving force of crystallization, $\Delta\mu$, and external pressure, p

The difference, $\Delta\mu$, in the chemical potentials of the ambient and the newly formed phase is the thermodynamic driving force of crystallization. It enters the work of nucleus formation and determines the frequency of melt/crystal transitions of the ambient phase molecules (see [20]). In deriving the necessary formalism we follow the standard procedure described in detail by Gutzow and Schmelzer [20]. We should note here that the temperature and pressure dependence of this thermodynamic function follows directly from its full differential which reads as:

$$d(\Delta\mu) = -\Delta S dT + \Delta V dP$$

for a single component system.

Integrating from $T = T_m(O)$, $P = P_o$ (where $\Delta\mu \equiv \Delta\mu(T_m, P_o) \equiv 0$) we obtain:

$$\Delta\mu(P, T) = -\int_{T_m(o)}^{T} \Delta S(T, P_o)\, dT + \int_{P_o}^{P} \Delta V(T_m, P)\, dP \tag{6}$$

With the already introduced temperature and pressure non-dependent integrand values ($\Delta V \equiv \Delta V(T, P) = \Delta V_m$ and $\Delta S_m(T, P_o) \equiv \Delta S_m$) it follows that:

$$\Delta\mu(T, P) \cong \Delta S_m(T_m - T) + \Delta V_m(P - P_o) \tag{7}$$

The first term in Equation 7 is the well known Thomson approximation:

$$\Delta\mu(T, P_o) \equiv \Delta\mu(O) = \Delta S_m \Delta T_m \tag{8}$$

giving the value of $\Delta\mu$ at normal pressure, where $\Delta T = (T_m(O) - T)$ is the undercooling with respect to $T_m(O)$. We have previously discussed a number of more accurate approximations for $\Delta\mu(T, P_o)$ [19, 20]. Here we prefer the simplest expression, Equation 8, in order to obtain more transparent results when analysing the kinetic dependences in the following sections. Equation 7 can also be written as:

$$\Delta\mu(T, P) = \Delta\mu(0) f_2(P) \tag{9}$$

where using Equation 2 we obtain:

$$f_2(P) \equiv \left[1 + \frac{\Delta V_m(P - P_o)}{\Delta S_m \Delta T}\right] = \left\{1 + \frac{T_m(p) - T_m(O)}{T_m(O) - T}\right\} \tag{10}$$

From the right hand side of the last equation it is evident that significant pressure dependent corrections in $\Delta\mu(T, P)$ (i.e., $f_2(P) \gg 1$) are only necessary either at small undercoolings (at $[T_m(O) - T] \ll [T_m(P) - T_m(O)]$) or at extremely high $\Delta V_m/\Delta S_m$ values.

It is also useful to combine Equations 7 and 2 as follows:

$$\Delta\mu(P, T) \cong \Delta S_m[T_m(P) - T] \tag{11}$$

expressing $\Delta\mu(T, P)$ in terms of the undercooling with respect to $T_m(P)$.

2.3. Pressure dependence of the melt/crystal interface energy, σ

When considering the thermodynamics of the undercooled melt/crystal interface and the corresponding specific surface energy, σ, we have to account for the following:

(i) At $\Delta\mu \geqslant 0$, only a crystalline cluster having a radius of curvature r determined by the Thomson–Gibbs equation:

$$r = 2\sigma/\Delta\mu \tag{12}$$

(i.e., the critical cluster or nucleus) is in thermodynamic equilibrium with the undercooled melt. Adopting, as frequently done (see [21–24]), the concept of an interface phase, intermediate between the two bulk phases (f) and (c), we have to restrict our considerations only to sufficiently large clusters, so that division of their building units into a surface and bulk part should still be possible. Moreover, we assume that the effect of curvature on σ can be neglected (i.e., it could be expected that $\sigma_{(r)} \cong$ constant $= \sigma_\infty$, as assumed in the classical capillary formulation of the nucleation theory.) The subscript, (σ), denotes the symbols of the thermodynamic parameters of this hypothetical interface phase.

For the particular case of crystalline clusters, the conventional provision of a quasi-isotropic spherical crystallite is usually made.

(ii) Recalling Gibbs' phase rule, it is evident that a two-phase single component system becomes nonvariant if a plain interface phase (i.e., with $r \to \infty$) between two infinitely large phases (f) and (c) is assumed. However, in our case of $\Delta\mu > 0$ and for the model of a crystalline phase (c) of finite radius, r, within an infinitely large liquid (f), the system attains an additional degree of freedom [22]. Moreover, by applying an external pressure, P, on the liquid

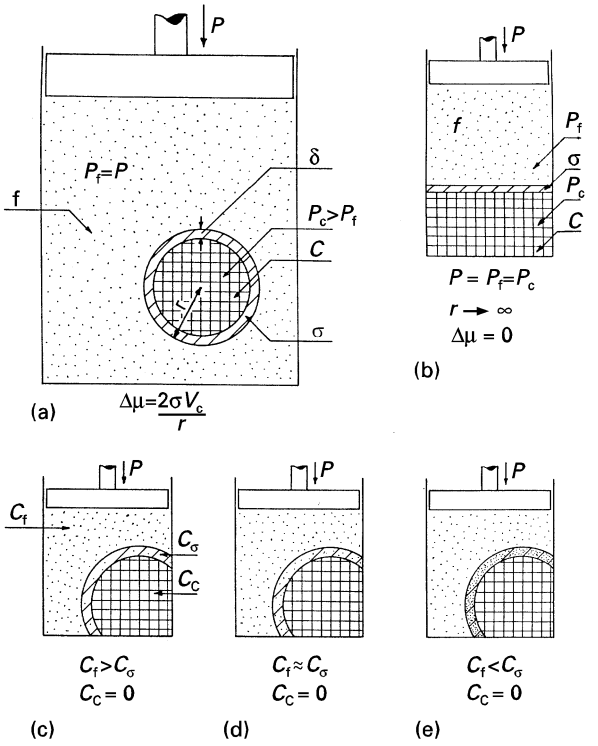

Figure 2 Thermodynamic model employed in calculating $(\partial\sigma/\partial p)_T$ and $(\partial\sigma/\partial_T)_p$. (a) A crystalline nucleus of radius r of the new crystalline phase (c) within the ambient phase (the undercooled liquid (f)); inbetween: the interfacial layer of the σ-phase with a thickness δ. An external pressure $P > P_o$ is applied on the whole system resulting in $P_f = P$ in the liquid and $P_c = P_f + 2\sigma/r$ in the cluster. Here $\Delta\mu = \mu_c(r) - \mu_f(\infty) = 2\sigma V_c/r$. This model corresponds to Equations 13 and 14. (b) For a plane interface ($r \to \infty$), $P = P_f = P_c$ and $\Delta\mu = 0$ (liquid at melting point T_m). Lower row of pictures: influence of concentration C of the second component (surfactant) in undercooled ($\Delta\mu > 0$) pseudo binary liquid with surfactant insoluble in the crystal (i.e., $C_c = 0$). (c) Concentration of surfactant in the interface layer intermediate between f and C (i.e., $C_f > C_\sigma > C_c$), linear approximation possible; (d) no enrichment of the second component in the interface ($C_f \approx C_\sigma > C_c = 0$) and (e) typical surfactant action of the second component: $C_\sigma > C_f > C_c = 0$.

containing the crystallite (see Fig. 2(a–e)), we have to take into consideration that the pressure, P_c, inside the crystallite would differ from that in the liquid, (P_f), the difference being determined via Equation 12. Thus here, and in deriving the kinetics of nucleation, we refer to P as being in fact $P = P_f$. If we assume that $P_f = P = \text{const.}$, the pressure, P_c, inside the cluster can still change (e.g., if the temperature of the whole system is changed). In Russanov's excellent monograph [22], the above proposed thermodynamic model for melt nucleation at $P = P_f = \text{const.}$ is treated in great detail. We have used here directly a number of results from this work [22] and refer the interested reader to the original.

(iii) We restrict our quantitative considerations to the case of a single component undercooled melt/crystal system. However, it is known that often even minor additives (surfactants) can be absorbed into the interface layer leading to dramatic changes in σ and, as will be discussed below, altering even the sign of both the $(d\sigma/dT)_P$ and $(d\sigma/dP)_T$ dependences. Moreover, it is possible that even seemingly simple single component melts contain different structural units. Some of the latter can have increased affinity to the crystalline structure and thus be present in higher concentrations in the interface layer. Problems of this kind, however, can be discussed here only in qualitative terms. For the single component case of an $(f)/(c)$ interface, according to Russanov (see Section 3. VIII. of his book [22]), it follows:

$$m_o(d\sigma/dT)_p = -[(S_\sigma - S_f) + (V_c^\sigma/V_c)\Delta S] \qquad (13)$$

and

$$m_o(d\sigma/dT)_T = [(V_\sigma - V_c)V_f - (V_f - V_c)V_f^\sigma](1/V_c) \qquad (14)$$

In Russanov's treatment and in the above formulae, three different values of the molar volumes of the system's building units are considered: (a) corresponding to both bulk phases (V_f, V_c); (b) to the crystal/melt interface layer (V_σ) and (c) to the layer in one of the phases adhering to the σ-phase (V_c^σ, V_f^σ).

If the interface phase is considered to be a monolayer, m_o, in above equations corresponds to the projected area of the molecular volume, V_c [21–23], i.e.,

$$m_o \cong [V_c]^{2/3} N_A^{1/3} \qquad (15)$$

where N_A is Avogadro's number of $V_c \approx V_m^c (T = T_m)$.

For the values of the entropy and molar volumes in the interface layer (S_σ and V_σ) in Equations 13 and 14 it can be assumed that they are in general in between those of the respective bulk properties (see [21, 22]) (i.e., $S_c \leqslant S_\sigma \leqslant S_f$ and $V_c \leqslant V_\sigma \leqslant V_f$). It can also be assumed that the values of V_c^σ and V_f^σ are in general fairly close (or even equal) to V_c and V_f, respectively.

Proceeding as in our previous publications [24–26], i.e., by introducing an adjustable dimensionless parameter ($0 \leqslant x \leqslant 1$) we can determine V_σ by linear interpolation as being equal to:

$$V_\sigma \approx (1 - x)V_f + xV_c \qquad (16)$$

If we account for the V_c^σ and V_f^σ values deviating from V_c and V_f, we can write:

$$V_f^\sigma \cong ZV_f \qquad \text{where } (V_c/V_f) \leqslant Z \leqslant 1 \qquad (17)$$

and

$$V_c^\sigma \cong YV_c \quad \text{where } (V_f/V_c) \leqslant Y = 1/Z \geqslant 1 \qquad (18)$$

In this way, V_c^σ and V_f^σ can take any value between V_c and V_f, the provision $Z \approx 1$ and $Y \approx 1$ being, however, most probable. Depending on the liquid model assumed, the configurational entropy of the melt, defined as the entropy difference, $\Delta S = (S_f - S_c)$, is a more or less complex logarithmic function of the relative free volume, ϑ, of the liquid, which can be defined as [19, 20]:

$$\vartheta = \Delta V/V_f \qquad \text{with } \Delta V = (V_f - V_c) \qquad (19)$$

For undercooled liquids (i.e., for $\vartheta < 0.05$–0.10), the simple expression:

$$\Delta S \approx 3R\vartheta \qquad (20)$$

can be derived by developing the respectively logarithmic functions as truncated Taylor series (see [20]).

Moreover, for undercooled liquids $V_f \approx V_c$ and Equation 20 can be also written in the already employed form of Equation 3. The above considerations give also the possibility of estimating S_σ in Equation 13.

By analogy to Equation 19 we can define the relative free volume, ϑ_σ, in the interface layer as:

$$\vartheta_\sigma = (V_\sigma - V_c)/V_\sigma \tag{21}$$

and its configurational entropy, $\Delta S_\sigma = S_\sigma - S_c$, as:

$$\Delta S_\sigma \approx 3R\,\vartheta_\sigma \tag{22}$$

In this way, by substituting the previously estimated values for V_σ, V_f^σ and V_c^σ into Equation 14 we obtain:

$$(d\sigma/dP)_p \cong -(K_o/m_o)\Delta V \tag{23}$$

where

$$K_o = [x - (1 - Z)](V_f/V_c)$$

With the same estimations substituted into Equations 13, 21 and 22 we obtain:

$$(d\sigma/dT)_p \cong -(g_o/m_o)\Delta S \tag{24}$$

where $g_o = \{g^* - [1 - (1/Z)]\}$ and $g^* = (1 - x)/\{[1 + (V_c/V_f)\} - x\}$

Considering that in general $x \approx 0.5$ and $z \cong 1$, it is evident that $K_o > 0$ and thus Equation 23 means that (as far as a single component system is considered) $(d\sigma/dp)_T < 0$ is always to be expected for the melt crystal interface at $\Delta V > 0$. This is a very substantial result as it leads (see section 6) to an additional reduction of the thermodynamic barrier of nucleation, ΔW, under pressure. Thus a definite answer to the question posed in the paper of Uhlmann *et al.* [5] becomes possible. This result is also pleasing from a more general point of view as it gives (for cases where $\Delta V > 0$) the expected positive sign for the so called Tolman parameter, δ, which can be defined as:

$$\delta = -(d\sigma/dP)_T$$

This parameter appears in the $\sigma(r)$ dependences following from the general theory of surface phenomena ([20, 22, 27] and especially [28]). For $\Delta V < 0$ (i.e. for the water/ice case) on the contrary, $\delta < 0$ has been found (see evidence reported by Gorski [29]) and this follows also from the above considerations.

Considering that $V_c/V_f \approx 0.80$–0.95 it is also evident that the dimensionless factor, g_o, in Equation 24 is also substantially positive. As far as in Equation 24 values of $x \approx 0.5$ and the estimate $Z \approx 1$ are most probable (and so $g_o \approx g^*$), the possibility that $g_o = 0$ is generally also to be excluded. Thus for the melt/crystal interface it is to be expected that $(d\sigma/dT)_p < 0$ in correspondence with the vapour/liquid case and the well known Eötvös rule ([22, 23]). This result is also of significance in analysing the temperature dependence of ΔW and of the nucleation rates in melt crystallization. After integration of Equation 24 (assuming, as in the derivation of Equation 2 that $\Delta S \approx \text{constant} = \Delta S_m$) we obtain (see also [24]):

$$\sigma(T, P_o) \cong \sigma_o + (g_o/m_o)\Delta\mu(T, P_o) \tag{25}$$

The value of $\sigma_o \equiv \sigma(T, P_o)$ can be estimated using the Scapski–Turnbull formula (see literature cited in reference [24] as:

$$\sigma_o = \gamma_o \Delta S_m T_m/m_o \tag{26}$$

where $\gamma_o \approx 0.4$–0.6 is the dimensionless Stefan coefficient [20]. Under the identical assumption ($\Delta V = \text{constant}$) Equation 23 gives after integration:

$$\sigma(T, P) = \sigma(T, P_o) - (k_o/m_o)\Delta V\,(P - P_o) \tag{27}$$

where $\sigma(T, P_o)$ is determined by Equation 25.

We have mentioned that K_o in Equations 23 and 27 is substantially positive for a pure single component system. However, in two or multicomponent systems, as discussed below, $K_o < 0$ can also be expected.

In both cases ($K_o > 0$ and $K_o < 0$) we can write, considering Equation 26:

$$\sigma(T, P) = \sigma_o\left[1 + \frac{g_o}{\gamma_o}\frac{\Delta T}{T_m(O)} - \frac{K_o}{\gamma_o}\frac{\Delta V_m}{\Delta S_m T_m(O)}(P - P_o)\right] \tag{28}$$

However for the particular case of $K_o < 0$ (and assuming that $g_o \approx K_o = l_o$) with Equation 7 it follows also that:

$$\sigma(T, P) = \sigma_o[1 + (l_o/\gamma_o)\,\Delta\mu\,(T, P)] \tag{29}$$

In both cases ($K_o > 0$ and $K_o < 0$) we can introduce a new coefficient $f_i(P)$ with:

$$\sigma(T, P) = \sigma(T, P_o) f_3(P) \tag{30}$$

where

$$f_3(P) = \left[1 - \frac{K_o}{\gamma_o}\frac{\Delta V_m}{\Delta S_m T_m}(P - P_o)\right] \tag{31}$$

Using Equation 3, Equation 28 can be written as:

$$\sigma(T, P) \approx \sigma(T, P_o)\,[1 - (K_o/\gamma_o)T_m(P)] \tag{32}$$

For two and multicomponent systems, an additional factor, χ_i, has to be introduced into Equations multiplying the ΔS term in Equation 13 and the $(V_f - V_c)$ term in Equation 14. The factor χ_i depends on the concentration, C_i, of the additional components in the liquid, (C_{if}), in the crystalline phase, (C_{ic}), and in the interface phase, ($C_{i\sigma}$). For a quasi-two component system [22], $\chi_i = \chi_2$ which has the structure:

$$\chi_2 = (C_\sigma - C_c)/(C_f - C_c) \tag{33}$$

In most cases of melt crystallization, the assumption $C_c \approx 0$ can be made. In this case the influence of χ_2 depends on the ratio C_σ/C_f. Here only in a very restricted number of cases an assumption similar to that given by Equation 16 (i.e., $C_c < C_\sigma < C_f$ and subsequent linear interpolation) can be made. On the contrary, of the three possibilities: $C_\sigma/C_f = 0$, $C_\sigma/C_f \approx 1$, and $C_\sigma/C_f \gg 1$ (see Fig. 2(a–e)) the last one, corresponding to the introduction of a typical surfactant, is the most striking one as it leads with certainty to a change not only in the value, but also in the sign of both the $(d\sigma/dP)_T$ and the $(d\sigma/dT)_p$ dependences given with Equations 23 and 24 (i.e., both $K_o < 0$ and $g_o < 0$ can be expected).

Recalling the possibility of the adsorption of different structural units even in seemingly simple systems previously mentioned, it is evident that the results following from Equations 23 and 24 are restricted in certain respects.

There is no direct measurement or any experimental evidence even for the sign of the $\sigma(P)$ and $\sigma(T)$ dependences of the melt/crystal case. For the vapour (v)/liquid (f) case there are plenty of measurements giving $d\sigma_{V/f}/dT < 0$ ([21, 22]). However, the known $\sigma_{V/f}(P)$ dependences are obtained from measurements under pressure applied to the system by more or less soluble gases. Thus a second component is introduced and consequently considerable χ_2 influences are to be expected [22, 23, 27, 28]. Only in some cases (e.g., in the H_2O/He system) the negative value of the $(d\sigma/dP)_T$ dependence for the vapour/liquid case can be experimentally verified [23, 27].

The significant point here is that Equation 24 confirms (for $K_o > 0$) a theoretical possibility for a decrease in σ upon increased pressure and thus a new possibility for decreasing ΔW and hence increasing the rate of nucleation in melt crystallization. This pressure dependent effect could be, generally speaking, of significance to any process of nucleation. Of particular interest in this respect are cases of vapour condensation in which a vapour/foreign gas system is subjected to various pressures: here the respective $(d\sigma/dP)_T$ values are known from measurements described in detail in references [22, 23, 27]. However, in melt crystallization we have to rely only on estimates given by Equations 23 and 24. An experimental estimate in this respect, following from the shift of the maximum nucleation rates, can also be made as discussed in Section 5.

3. Dependence of melt viscosity and of the kinetic factors of crystallization on pressure

There are different ways to introduce the necessary kinetic factors into the formalism describing melt crystallization: via the impingement rate, (z_o), of ambient phase molecules, through the coefficient of self-diffusion, (D_o), of the melt's building units or by the time of molecular relaxation (τ_R) of the melt [20].

In fact, in each of these cases a dependence equivalent to the Stokes–Einstein formula [30] is used:

$$D_o = kT/d_o\eta \tag{34}$$

relating D_o (or the other kinetic characteristics of the melt) to the viscosity, η, i.e., its only directly measurable kinetic parameter. In the above equation d_o, denotes the mean intermolecular distance in the liquid ($d_o \approx (V_m/N_A)^{1/3}$).

The free volume model for liquids defines melt viscosity as being determined by two probabilities: of activating a molecule (it depends on the nearly constant activation energy, U_o) and of finding an appropriate free volume for jumping of the molecule [31]. The latter probability is proportional to $\exp[-B_o/\vartheta]$. Consequently, the Macedo–Litovitz equation follows [32] (see also [19, 20, 24, 33]):

$$\eta(T, p_o) = A_o \exp[U_o/RT] \exp[B_o/\vartheta] \tag{35}$$

where ϑ is the already introduced relative free volume of the melt and, B_o, is a kinetic factor depending on the complexity of the molecules. For the simplest liquids (like molten metals or liquid Ar) $B_o \approx 1$; for more or less complex building units, B_o values ranging from 4 to 6 can be expected [24, 33].

With Equation 19, rewritten for an undercooled melt where $V_f \approx V_c$, the free volume, ΔV, of the melt (corresponding approximately to the van der Waals free volume ($V_f - b_o$) becomes equal to $\Delta V \approx V_o\vartheta$. Introducing an appropriate equation of state corresponding to the already employed free volume model for the liquid, we can determine the $\eta(T)$ dependence via Equation 35. A suitable choice would be a modification of the van der Waals equation proposed by Tumlirz [34] for liquids:

$$(P + \Pi_o)(V_f - b_o) = RT \tag{36}$$

where Π_o is the internal pressure of the liquid ($\Pi_o \sim a_o/V_f$) and b_o is the van der Waals occupied volume ($b_o \sim V_c$).

With Equation 36 introduced into Equation 35 we obtain:

$$\eta(T, P) = A \exp[U_o/RT] \exp[(B_oV_c/RT)(P + \Pi_o)] \tag{37}$$

Other attempts to derive a similar $\eta(p)$ dependence may be found in the literature [30] and [35]. The above results also correspond to an empirical dependence (Suge's formula, [34]):

$$\log P = A^{\#} + B^{\#}p \tag{38}$$

known to fairly well describe the pressure dependence of viscosity. The coefficients in Equation 38 are thus determined as:

$$A^{\#} = (U_o + \Pi_oP_oV_c)/2.3\,RT, \quad B^{\#} = B_oV_c/2.3\,RT \tag{39}$$

Redefining $\eta(T, P_o)$ with Equation 36 as:

$$\eta(T, P_o) = A_o \exp(U_o/RT) \exp[B_oV_c(P + \Pi_o)/RT] \tag{40}$$

we obtain:

$$\eta(T, P) = \eta(T, P_o) \exp[(B_oV_c/RT)(P - P_o)] \tag{41}$$

Denoting the overall activation energy at $P = P_o$ as:

$$U(T, P_o) = U_o[1 + (B_oV_c/U_o)(P - P_o)] \tag{42}$$

we can also write for an increased pressure P that:

$$\eta(T, P) = A_o \exp[U(P, T)/RT] \tag{43}$$

Here

$$U(T, P) = U(T, P_o) f_4(P) \tag{44}$$

denotes the overall activation energy corresponding to (T, P) and the dimensionless coefficient:

$$f_4(P) = \{1 + [B_oV_c/U(T, P_o)](P - P_o)\} \tag{45}$$

corresponds to the previously introduced factors f_i (see Equations 5, 9 and 30).

According to Equations 36, 44 and 45 we can also write:

$$[\mathrm{d}\log\eta(T,P)/\mathrm{d}P]_T = d[f_4(P)]/\mathrm{d}P = B_o V_c/2.3\,RT \tag{46}$$

Experimental evidence is in good agreement with Equation 41. Figs 3, 4 and 5 show examples in this respect, illustrating the influence of pressure on viscosity for two typical glassforming melts (B_2O_3 and Se according to data from references [36] and [37]).

The d log η/dp values following from Fig. 3 give $(B_o V_c/2.3R) \approx 5.6 \times 10^{-6}\,\mathrm{kPa}^{-1}$ for the B_2O_3 system. A comparison with the theoretically expected value ($1.9 \times 10^{-6}\,\mathrm{kPa}^{-1}$) gives a very reasonable assessment for the complexity of B_2O_3 melts ($B_o = 3$). From Fig. 4 the value for $B_o V_c/2.3R$ for Se melts turns out to be $\sim 8.5 \times 10^{-6}\,\mathrm{kPa}^{-1}$. A juxtaposition with the expected value gives $B_o \approx 1$. The mean activation energy, $U(T,P)$, for Se melts in the temperature range of 250–350 °C, as determined from Fig. 5, turns out to be $\sim 70\,\mathrm{kJ\,mol}^{-1}$. This value of $U(T,P)$ is practically unaffected in the pressure range from P_o(0.1 MPa) to 0.4 GPa: the respective $(p - p_o)V_c$ values are too small in this pressure range. Thus Fig. 5 and simple estimates show that a measurable change in the activation energy – above the experimental scatter – should be expected for inorganic melts only at $p \geqslant 1$ GPa.

Fig. 6 presents the log η versus p curves (for respective data see reference [37]) for a typical molecular liquid (ethanol) with $\Delta V > 0$. They allow for an interesting comparison with the change in η for a molecular substance (H_2O) with $\Delta V < 0$ (Fig. 7 according to

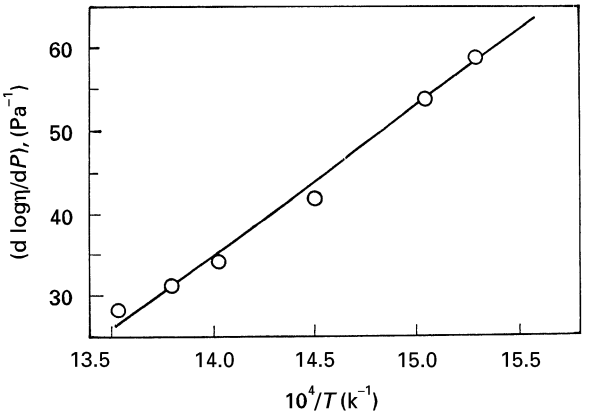

Figure 3 Pressure dependence of the viscosity of B_2O_3 melts. Temperature dependence of the coefficient d [log η]/dp according to the data provided by Sperry and Mackenzie [36].

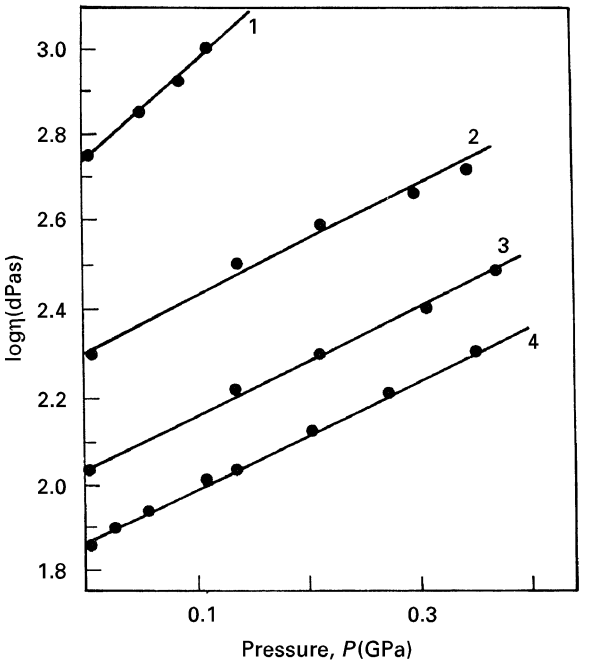

Figure 4 Pressure dependence of the viscosity η of Se-melts at different temperatures ((1) 260 °C, (2) 300 °C, (3) 330 °C and (4) 350 °C) according to experimental data summarized in the reference literature [37].

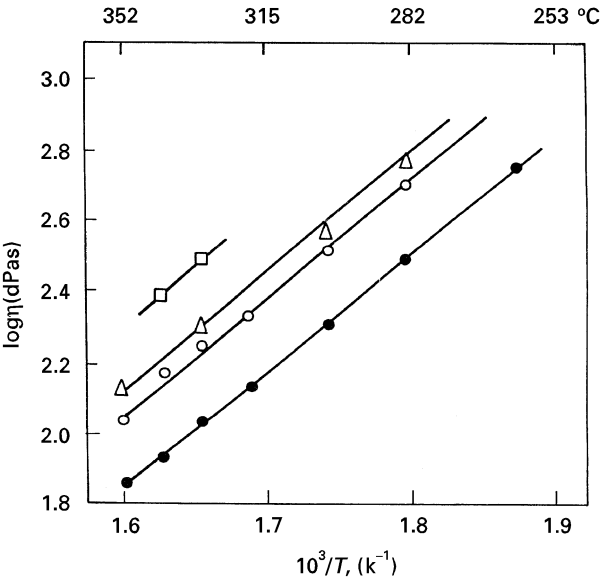

Figure 5 Temperature dependence of the viscosity of Se melts under pressure. The same experimental data as in Fig. 4 in coordinates of log η versus $1/T$ at different pressures: (□) 0.37 GPa; (△) 0.20 GPa; (○) at 0.135 GPa and (●) at atmospheric pressure (0.1 MPa).

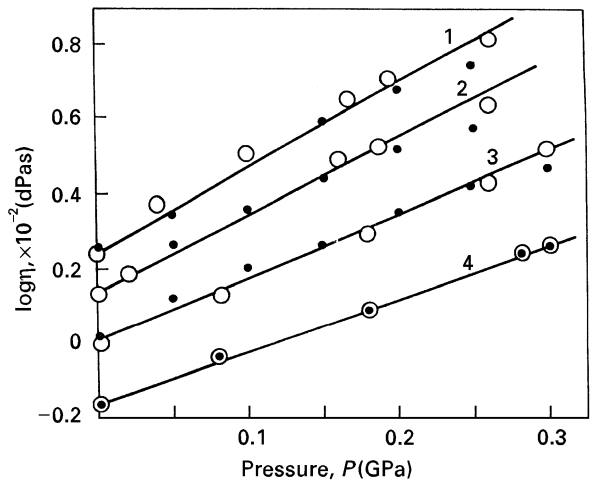

Figure 6 Pressure dependence of the viscosity η of ethyl alcohol at (1) 0 °C; (2) 15 °C; (3) 30 °C and (4) 53.5 °C according to reference data from [37]. Black points and open circles: two sets of measurements by different authors.

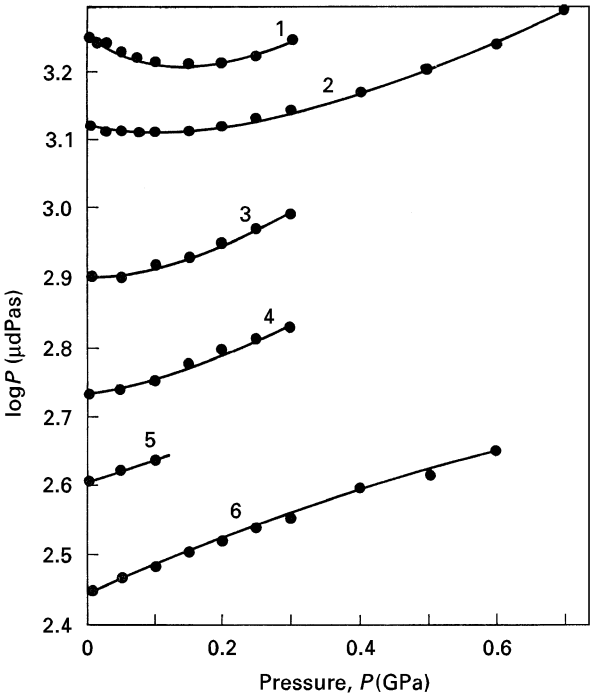

Figure 7 Pressure dependence of the viscosity of water at (1) 0 °C; (2) 10 °C; (3) 30 °C; (4) 50 °C; (5) 70 °C and (6) 100 °C from reference data summarized in [37]. Note the initially negative slope of the log η(*P*) curves at lower pressures for temperatures from 0° to 10 °C.

data from reference [38]). At low pressures and temperatures close to the well known density anomaly of water, the coefficient $[\mathrm{d}\log\eta/\mathrm{d}p]_T$ has negative values. This would be expected if a negative free volume $(V_f - V_c) < 0$ is formally introduced into Equations 19 and 35. Of course, such a formal treatment faces difficulties of a very general nature, if the assumptions of the simple free volume model are accounted for. It is obvious, however, that when considering the crystallization phenomena in liquid/crystal systems with $\Delta V < 0$, a behaviour of the log η versus *p* dependence similar to the one shown in Fig. 7 for water should also be considered.

4. Kinetics of crystallization under hydrostatic pressure: basic dependences

The results of many years of theoretical development in the field of nucleation and growth kinetics and the contribution of many authors can be summarized in a set of kinetic equations giving the dependence of the three basic parameters of the crystallization process in an undercooled melt (nucleation rate, *I*, crystal growth rate, *g*, and non-steady-state time lag, $\tau^{\#}$) on temperature, *T*, and the thermodynamic driving force of crystallization, Δμ. The more or less standard way of deriving these kinetic dependences (for $P = P_o$) have been described many times in the literature [20, 39, 40]. Taking into account the results in the preceding paragraphs and using the $f_i(P)$ factors introduced there, and the formalism employed in reference [20] (see also references [24, 33, 41]), one can easily derive the corresponding expressions for an increased pressure, *P*. The results thus obtained can be expressed in a generalized form as follows:

$$I_{SS}(T,P) = \mathrm{const}_1 \exp[-U(T,P_o)f_4(p)] \times \exp[-\Delta W(T,P)/kT] \quad (47)$$

for the steady-state nucleation rate:

$$g = \mathrm{const}_2 \exp[-U(T,P_o)f_4(P)]\,\Omega[-\Delta\mu f_3(P)] \quad (48)$$

for every one of the three basic mechanisms of crystal growth (see [20, 40]) and

$$\tau^{\#} = \mathrm{const}_3\{\sigma_o f_3(P)/[\Delta\mu_o f_2(P)]^2\}\exp[U(T,P_o)f_4(P)] \quad (49)$$

for the non-steady-state time lag.

The physical meaning of the above introduced three parameters is well known from the generalized non-steady-state formulation of the theory and is described in detail in the literature [20, 24, 41]. In the above formulae, $f_i(P)$, denote the functions given with Equations 5, 9, 30 and 44. $\Delta W(T,P)$ indicates the thermodynamic barrier to nucleation at pressure *P*:

$$\Delta W(T,P) = \{\Delta W_o[f_3(P)]^3\}/[f_2(P)]^2 \quad (50)$$

and ΔW_o gives the same barrier at (T,P_o) which according to a well known classical result (see [20, 39, 40]) can be expressed as:

$$\Delta W_o = (\omega_3\sigma_o^3 V_c^2)/\Delta\mu_o^2 \quad (51)$$

The geometric factor in the above formula is $\omega_3 = (16\pi/3)$ in the isotropic approximation; σ_o, $\Delta\mu_o$ refer to the normal pressure case. Expressing σ_o by Equation 26 and $\Delta\mu_o$ by Equation 8 we can write ΔW_o in the form (see also [33]):

$$\Delta W_o \cong [(\omega_3\gamma_o^3\Delta S_m T_m)/N_A](T_m/\Delta T)^2. \quad (52)$$

where ΔT is the undercooling $[T_m(o) - T]$.

In the rate of crystal growth equation, Ω and $[\Delta\mu(P,T)]$ denote different $\Delta\mu(P,T)$ functions, their concrete form being determined by the particular mechanism of growth (see [20, 40]). For the above mentioned basic mechanisms of growth we have to write:

$$\Omega(T,P) = \beta_o\Delta\mu f_2(P) \quad (53)$$

for the case of "normal" mechanism:

$$\Omega(T,P) = \beta_S(\Delta\mu_o f_2(P)]^2\,\sigma_o f_3(P) \quad (54)$$

for spiral growth, and:

$$\Omega(T,P) = \beta_d \exp[-\Delta W_2(T,P)/kT] \quad (55)$$

for growth determined by two-dimensional nucleation.

In the above equations β_o, β_S and β_d are specific (*T* and Δμ-independent constants, see [20, 40]), the first one being equal to the relative number of growth sites on the crystal face. The expression:

$$\Delta W_2(T,P) = \{\omega_2\sigma_0^2 V_c d_c[f_3(P)]^2\}/[\Delta\mu_o f_2(P)] \quad (56)$$

gives the work of two-dimensional nucleation (see [20, 40]) under pressure *P*, the geometric constant

here being $\omega_2 = \pi$ (assuming again circular symmetry). With d_c in Equation 56 we denote the mean intermolecular distance in the crystal (i.e., $d_c \approx (V_c/N_A)^{1/3}$).

The significant thermodynamic factors in the above formulae are the two nucleation barriers (Equations 50, 52 and 56) determining three and two-dimensional nucleation, respectively. In deriving the above formalism only two common assumptions are made corresponding to the classical capillary model of nucleation: that the specific interface energy σ_o (or $\sigma_o(P)$, respectively) does not depend on the radius r of the critical cluster and that the crystal is incompressible (i.e., V_c = constant as already assumed in section 2). The first kinetic exponential term in Equations 47–49 introduced via the Stokes–Einstein equation [34] assuming for $\eta(P, T)$ the temperature dependence given with Equations 43 and 44, the coefficient $f_4(P)$ being determined by Equation 45.

It is seen that the three crystallization parameters (I_{ss}, g and $\tau^{\#}$) depend in very different ways on the $f_i(P)$ coefficients and thus on pressure. The exponential terms connected with the viscosity (i.e., with $f_4(P)$) determine decreasing nucleation and growth rates and increasing time lags with increasing P values. On the contrary, the $\Delta\mu$ correcting term $f_2(P)$ is involved in such a way in the rate equations that (at $\Delta V > 0$) I_{SS} and g increase; thus $f_2(P)$ and $f_4(P)$ have an opposite effect on the kinetics of crystallization. According to the more general Zel'dovish formulation of the theory (see [20, 24, 41, 42]), the time dependence, $I(t)$, of the nucleation rate is determined if an approximate solution of the Zel'dovich–Frenkel differential equation is adopted. Choosing here the simplest solution given by Zel'dovich himself we have:

$$I(t) = I_{SS}(T, P) \exp[-\tau^{\#}(T, P)/t] \qquad (57)$$

where $I_{SS}(T, P)$ and $\tau^{\#}(T, P)$ are defined by Equations 47 and 49. The increased $\tau^{\#}$ and (in most cases) decreased I_{SS} values should in general shift the I dependence in the way shown in Fig. 8(a–c). The structure of Equation 49 is such that the $f_4(P)$ function in the exponent leads (at $\Delta V > 0$) always to an increase in $\tau^{\#}$. As a rule for small ΔV values a decrease in I_{SS} is to be expected and only for extremely high ΔV values increased I_{SS} values are to be anticipated (see next Chapter). More exact solutions to the problems of non-steady-state kinetics of nucleation are discussed in the literature (see [20, 41, 42] and the references cited there).

The kinetics of overall crystallization in melts is best characterized by the time, t_c, needed for a given degree of crystallization, α_c, to be reached. Adopting again the simplest solution of the non-steady-state Avrami kinetics proposed in reference [43] (i.e., a $\tau^{\#}$ shift along the t-axis, see also references [20, 24]) we obtain:

$$t_c(T, P) \cong b_o \tau^{\#}(T, P) + \alpha_c^{1/4} / [(\omega_3/4) I_{SS}(T, P) g^3(T, P)]^{1/4} \qquad (58)$$

if a tridimensional growth model is considered (i.e., an Avrami coefficient of $n = 4$). The structure of the already discussed dependences determining the three basic crystallization parameters ($I_{SS}(T, P)$, $\tau^{\#}(T, P)$ and $g(T, P)$) in Equation 58 is such that in general an increase of the $\tau^{\#}$ value and a shift of the $\alpha(t)$ curve along the t-axis to higher t values is to be expected under increased pressure.

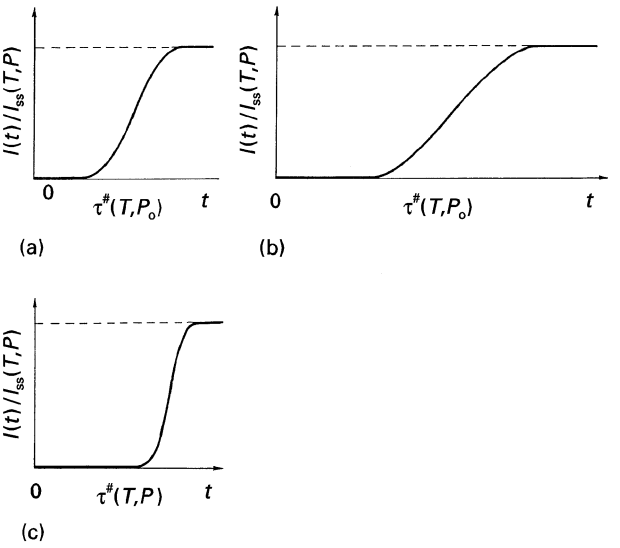

Figure 8 Nucleation kinetics in melt crystallization under normal pressure and under increased pressures, at a constant temperature, according to Equation 57. (a) $I(t)$ course at normal pressure; (b) increased pressure at $\Delta V/V_c < 0.05$; (c) increased pressure at $\Delta V/V_c > 0.10$.

Recalling Equations 47–50 it is evident that Equation 58 can also be written as:

$$\log(t_c(T, P)] = \text{const.} + (1/2.3RT)\{U(T, P_0) f_4(P) + [1\Delta W_o f_3(P)/4 f_2(P)]\} + 1/4 \log[(\alpha_c)/\Omega(\Delta\mu P, T) \qquad (59)$$

At high undercoolings (i.e., in the vicinity of the glass transformation temperature, T_g) $U_o(T, P)$ is considerably higher than ΔW_o and thus the dependence of $\log t_c$ on $f_4(P)$ should surpass all other influences.

5. Melt crystallization under hydrostatic pressure: possibilities and limitations

An inspection of Equations 47 and 50 accounting for the structure of the respective $f_i(P)$ functions shows that the possible effect of a pressure reduced nucleation barrier $\Delta W(P, T)$ (at $f_2(P) > 1$, $f_3(P) < 1$, i.e., at $\Delta V > 0$ and $(\partial\sigma/\partial p)_T < 0$) may be compensated (or even overcompensated) by the pressure increased kinetic factor $f_4(P)$. Thus the opposite effect of p on $U_o(T, P)$ and on $\Delta W(P, T)$ in Equation 47 determines a maximum in the $I_{SS}(T, P)$ versus P curve. The existence and the position of this maximum on the p-axis is determined by:

$$|\partial[\log I_{SS}(T, P)]/\partial p|_T = -|[U_o(T, P_o)/N_A][\partial f_4(P)/\partial P]|_T - \Delta W_o|[f_3(P)/f_2(P)]^2\{[3\partial f_3(P)/\partial P]|_T - |[2f_3(P)/f_2(P)][\partial f_2(P)/\partial P)|_T\} \leqslant 0 \qquad (60)$$

It is evident that for $\partial f_4(P)/\partial P > 0$ (at least at $\Delta V > 0$) such a maximum is to be expected (at $T < T_m(O)$) only for:

$$\{3\partial f_3(P)/\partial P - [2f_2(P)/f_2(P)]\,[\partial f_2(P)/\partial P]\}_T < 0 \tag{61}$$

i.e., when the kinetic and the thermodynamic terms in Equation 60 have opposite signs.

In the case when $f_3(P) \cong 1$, i.e., for $|(\partial\sigma/\partial p)|_T = 0$, Equation 60 gives, accounting for Equations 9 and 50, for the P value at the maximum of the $I_{SS}(P)|_T$ curve:

$$f_2(P) = \left(\frac{2\Delta W_o N_A \Delta V_m}{B_o V_c \Delta S_m \Delta T}\right)^{1/3} \tag{62}$$

With Equations 9 and 51, the above dependence gives:

$$(P_{max} - P_o) = (\Delta S_m T_m)\left(\frac{2\Delta W_o}{B_o}(\Delta V/V_c)\right)^{1/3} - (T_{m(o)} - T)/T_{m(o)}] \tag{63}$$

Such a ΔT dependent shift was in fact observed experimentally by Aziz *et al.* [6] in the crystallization of B_2O_3-melts under high pressures (Fig. 9). The same figure presents also the $T_m(P)$ dependence for B_2O_3 using the respective ΔV and ΔS_m values ($\Delta V_m = 13.7\ cm^3\ mol^{-1}$, $\Delta S_m = 31.8\ J\ K^{-1}$ mol, see [6]). At $(\partial\sigma/\partial p)_T < 0$, the $T_m(P)$ and P(max) versus T line should converge. For $(\partial\sigma/\partial p) > 0$ the reverse situation should be expected. In this way the course of the $P_{max}(T)$ versus P curve could give an indication for the character of the $(\partial\sigma/\partial p)$ dependence. The experimental evidence provided with B_2O_3 seems to suggest that $(\partial\sigma/\partial p) < 0$. However, both the $P_{max}(T)$ versus P and the $T_m(P)$ lines given in Fig. 9 are drawn only on the basis of three experimental points provided by Aziz *et al.* [6] and this is insufficient to allow a distinct conclusion in the above sense.

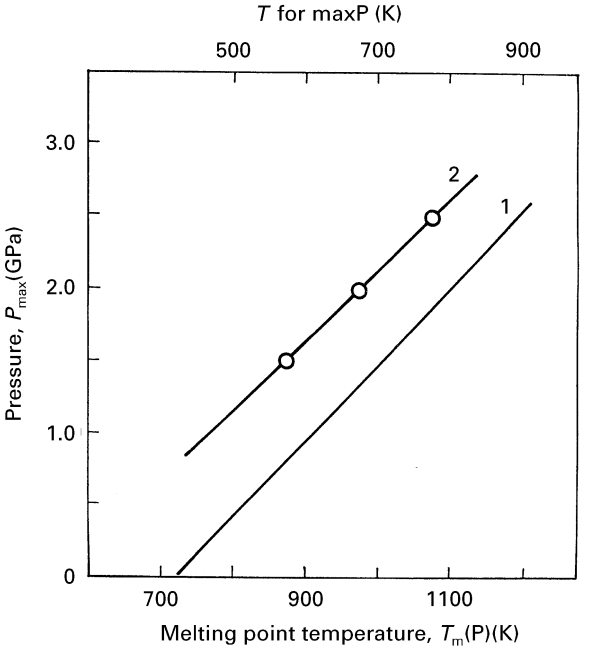

Figure 9 Data on the shift of the maximum rate of crystallization versus P curves at different temperatures T (indicated at figure top in K) and of pressure dependence of T_m (given in the bottom also in K) (1) $T_m(P)$ dependence in co-ordinates of P versus T (according to Equation 2) and ΔS_g and ΔV_g data from Aziz *et al.* [6]. (2) P_{max} versus T dependence according to experimental data of Aziz *et al.* [6].

It can also be seen from the above derivations that the maximum of the I_{SS} versus P curves shifts to higher pressures at greater relative volume changes ($\Delta V/V_c$) and for simpler melts (at $B_o \approx 1$). However, the appearance of a maximum on the $I_{SS}(P)|_T$ or $g(P)|_T$ curve does not imply that a catalytic effect is to be expected in melt crystallization under increased pressure. In order to determine the range of nucleation catalysis we have to consider the inequality:

$$2.3\,kT \log\{I_{SS}(P)/I_{SS}(P_o)\} = -[U(T,P_o)/N_A][f_4(c) - 1] - \Delta W_o\{[f_3(P)]^3/[f_2(P)^2 - 1\} \geqslant 0 \tag{64}$$

where $I_{SS}(P_o)$ and $I_{SS}(P)$ denote the nucleation rate at normal and at increased pressure, respectively.

Nucleation catalysis is to be expected only when:

$$[U(T,P_o)]/N_A\Delta W_o > \{[f_3(P)]^3/[f_2(P)]^2 - 1\}/[1 - f_4(P)] \tag{65}$$

With Equations 44, 45 and 52 the above condition can be written as:

$$0 < [\Delta T/T_m(O)]^2 < -[\omega\gamma_0^3/B_o V_c] \times \{[f_3(P)]^3/[f_2(P)]^2 - 1\} \tag{66}$$

For relatively low pressures (at $[\Delta V(P - P_o)/\Delta S_m] = q_o < 1$) and for $(\partial\sigma/\partial p)_T = 0$, the above inequality is fulfilled (for $\Delta T > 0$, i.e., at $T < T_m(O)$) when:

$$0 < \Delta T/T_m(O) < \left(\frac{2r_0^3 \Delta W_3 \Delta V}{B_0 V_c}\right)^{1/3} \tag{67}$$

With increasing pressure the $\Delta T/T_m(O)$ range of catalysed nucleation becomes narrower and at large $(P - P_o)$ values (i.e., at $q \gg 1$) we obtain:

$$0 < \Delta T/T_m(O) < \left(\frac{r_0^3 \Delta W_3 \Delta V}{B_0 V_c q_0}\right)^{1/2} \tag{68}$$

At $q_0 \to \infty$, this ΔT range shrinks to zero values. According to the above dependences the said $\Delta T/T_m(0)$ range depends mainly on the $\Delta V/V_c$ value. Thus for a glassforming melt like B_2O_3, where extremely high $\Delta V/V_c$ values are to be expected (according to Aziz *et al.* [6] $\Delta V/V_c = 0.20$), Equations 67 and 68 give $0 < [\Delta T/T_m] < 0.55$ at $B_o = 5$, and $0 < [\Delta T/T_m] < 0.1$ at $q = 20$. However, for typical glassforming systems like $Li_2O.2SiO_2$, where $\Delta V/V = 0.035$ at the same B_o value, we have to expect catalytic effect only at $0 < \Delta T/T_m(0) = 0.3$ and $0 < \Delta T/T_m(0) < 0.01$, respectively.

The above formulae speak for themselves: pressure induced nucleation catalysis is to be expected only for systems with relatively high or even extreme $\Delta V/V$ values and at medium pressures. At extreme pressures, the increase of the $f_4(P)$ factor nullifies not only the impact of $f_2(P)$, but also the possible effect of $f_3(P)$ (i.e., of the $\partial\sigma/\partial p$ decrease of $\Delta W(T,P)$). The overall result of pressure increase on nucleation kinetics is further restricted bearing in mind that at high undercoolings non-steady-state effects are becoming significant and τ increases exponentially with increasing

pressure P, and thus its catalyzing effect on the nucleation rate may be nullified (see Equation 57).

Equation (65) allows also for an analysis of the influence of pressure on nucleation in the case of $\Delta V < 0$. It can be shown that in this case practically no nucleation catalysis under pressure is possible (both $U(T, P)$ and $\Delta W(T, P)$ are increased).

The detailed analysis shows that at $(\partial\sigma/\partial p)_T > 0$ the $\Delta T/T_m(0)$ range of nucleation catalysis is considerably narrower as compared to the $(\partial\sigma/\partial p)_T = 0$ case. Pressure induced nucleation catalysis at $(\partial\sigma/\partial p)_T > 0$ is only possible at low pressures and at very low ΔT values. On the contrary, at $(\partial\sigma/\partial p)_T < 0$, the ΔT-range of possible nucleation catalysis is wider, e.g., in analogy to the foregoing results (see Equation 67), at relatively low pressures we obtain for the catalytic range:

$$\Delta T/T_m(O) \cong \left(\frac{2r_0^3 \Delta W_3 \Delta V}{B_0 V_c}\right)^{1/3} (k_o/\gamma_o + 1)^{1/3} \quad (69)$$

i.e., the previous result is extended by the factor $(k_o/\gamma_o + 1)^{1/3}$ where K_o is determined by Equation 23.

Even in the very first investigations on melt crystallization under hydrostatic pressure [1–3], an experimentally observed specific shift of the maximum and of the whole $I_{SS}(P)$ versus T or $g(p)$ versus T curves were reported.

In order to examine this effect (choosing as an example the $I_{SS}(P)$ versus T dependence) we have first to determine the position of the maximum T_{max} of the $I_{SS}(P)$ versus T curve from the derivative $\mathrm{d}[\log I_{SS}(T, P)]|_p/\mathrm{d}T$.

In employing an approximative method proposed years ago by Frenkel [44] to determine $T_{max}(P_o)$ (see reference [20]) we assume in differentiating the $\log I_{SS}(T, P)|_p$ dependence (cf. Equation 47) that the approximation $T \approx T_m(P)$ can be made in the additive term $\Delta W(P, T)/kT$ (cf. Equation 50). Supposing also that $T_{max}^2(P)\, T_m(P) \approx [T_m(P)]^3$, we obtain a Frenkel-like expression of the form:

$$[T_m(P) - T_{max}(P)] \cong \sigma_o f_3(P) \times \left(\frac{2\Delta W [V_c]^2 T_m(0) f_2(P)}{[\Delta S_m]^2 U(T, P_o) f_4(P)}\right)^{1/3} \quad (70)$$

Accounting for the already discussed dependence of $f_2(P)$ and $f_4(P)$ on P, the shift of T_{max} with $T_m(P_o)$ becomes obvious; the influence of $f_3(P)$ (and of possible $\sigma(P)$ effects) on $[T_m(P) - T_{max}(P)]$ is also evident. At $(\partial\sigma/\partial p) = 0$, i.e., at $f_3(P) = 1$, the effect of $f_2(P)$ and $f_4(P)$ is compensated and $[T_m(P) - T_{max}] \approx$ constant with increasing P values. At $(\partial\sigma/\partial p) < 0$, $[T_m(P) - T_{max}]$ becomes a decreasing function of P (see Fig. 10), determined by $f_3(P)$. For $(\partial\sigma/\partial p)_T > 0$, the reverse effect is to be expected. Thus the change of the above indicated difference with P is an indication of whether σ is a function of P and what is the actual direction of the change (i.e., $(\partial\sigma/\partial p) > 0$ or $(\partial\sigma/\partial p) < 0$).

From a more general point of view Equation 70 and Fig. 9 show that when pressure is applied (for systems with $\Delta V > 0$) the melt begins to crystallize and maximum crystallization rates are reached at elevated temperatures, where lower $\eta(P)$ values govern the kinetics of crystallization.

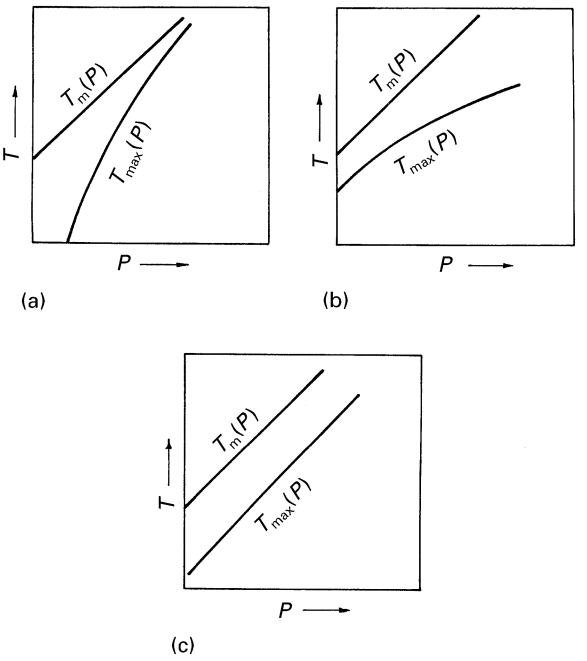

Figure 10 Dependence of T_{max} and T_m on pressure according to Equations 70 and 71. (a) for $(\partial\sigma/\partial p)_T < 0$; (b) for $(\partial\sigma/\partial p) > 0$; (c) for $(\partial\sigma/\partial p) = 0$.

The $T_{max}(P)$ shift predicted by Equation 70 is confirmed by the experimental evidence for the crystallization of $Li_2O \cdot 2SiO_2$ melts under pressure (see Burkhard and Russel [45] and Fig. 11. The same figure presents also the $T_m(P)$ dependence for $Li_2O \cdot 2SiO_2$ to be expected with the ΔV and ΔS values corresponding to this system ($T_m(P) = 1307\,\mathrm{K}$, $\Delta V = 2.0\,\mathrm{cm^3\,mole^{-1}}$ and $\Delta S_m = 41.4\,\mathrm{J\,K^{-1}\,mol^{-1}}$). The experimental results given by Burkhard and Russel [45] seem to confirm the conclusions made with Equations 23 and 24, namely that in melt crystallization, according to the analysis following from Equation 70, in general $(\partial\sigma/\partial p)_T < 0$, a result which, if confirmed for other cases, could be of exceptional significance.

A shift similar to that given with Equation 70 is also to be expected in the maximum of the $g(P)$ versus T curves for crystal growth under pressure. For the mechanism of crystal growth determined by two dimensional nucleation Equation 48 with Equations 55 and 56 gives:

$$T_m(P) - T_{max}(P) \cong \sigma_o f_3(P) \left(\frac{d_0 V_c T_m(0) f_2(P)}{[\Delta S_m] U(T, P_o) f_4(P)}\right)^{1/2} \quad (71)$$

For the dislocation mediated or normal growth mechanisms with Equations 48, 53 and 54 similar dependences are obtained:

$$T_m(P) - T_{max}(P) \cong \frac{2R[T_m(O) f_2(P)]^2}{U(T, P_o) f_4(P)} \quad (72)$$

as witnessed by the above equation derived for the dislocation growth mechanism. There are still no better confirmations of the above considerations than the

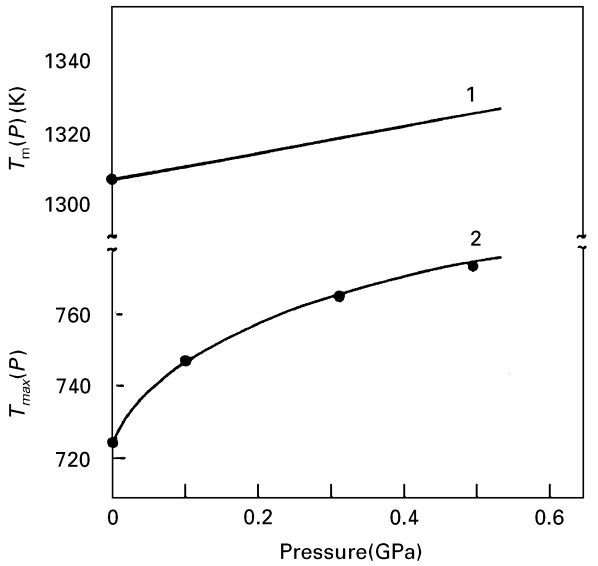

Figure 11 Shift of the melting point $T_m(P)$ and of the maximum rate of nucleation $T_{max}(P)$ in melt crystallization of $Li_2O \cdot 2SiO_2$ under pressure. (1) $T_m(P)$ dependence according to Equation 4 with ΔV and ΔS_m values given in the text; and (2) $T_{max}(P)$ dependence according to experimental data (black points) provided in reference [45].

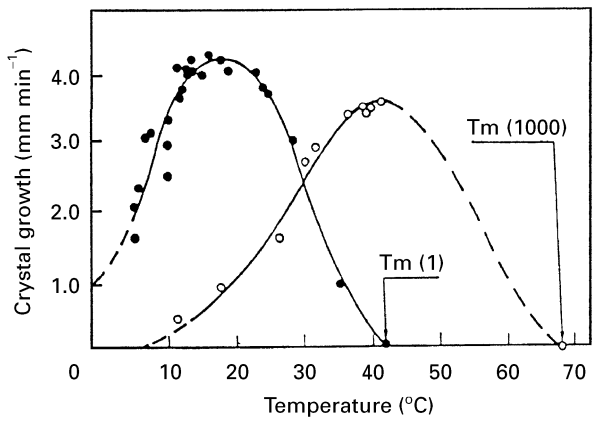

Figure 12 Shift of crystal growth versus curves under pressure according to the measurements performed by Hasselblatt [3]. Crystal growth/temperature curves of salol melts at normal pressure (1) and at 0.1 GPa (1000).

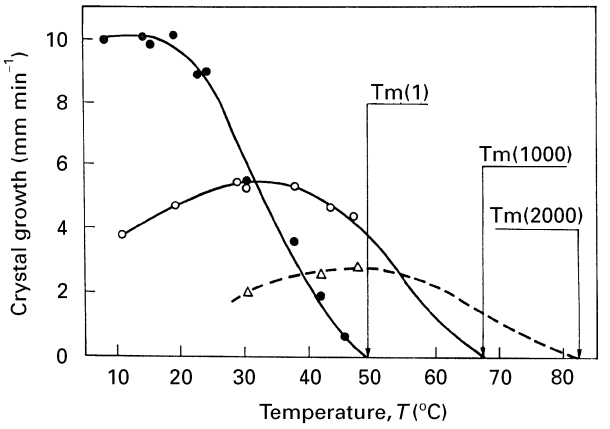

Figure 13 Shift of crystal growth curves in thymol melts at three different pressures: at normal pressure (1), at 0.1 GPa (1000), and at 0.2 GPa (2000).

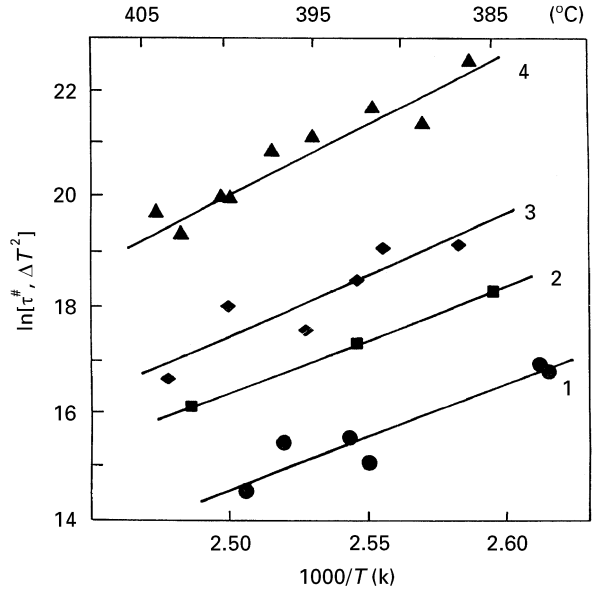

Figure 14 Shift of temperature dependence of non-steady-state induction periods $\tau^{\#}$ (determined from overall crystallization curves) for crystallization of Se melts under pressures of (1) 0.28 GPa; (2) 0.42 GPa; (3) 0.55 GPa and (4) 0.69 GPa. Ordinate and abscissa: according to Equation 49. Experimental results: by Mohan and Singh [47].

experimental data provided by Hasselblatt [3], according to which Figs. 12 and 13 have been drawn. These curves illustrate also in a very simple way the real nature of the influence of pressure on crystallization. They show that in fact not only the $T_{max}(P)$, but the whole $I_{SS}(P)$ or $g(P)$ versus T curves are shifted along the T-axis with $T_m(P)$.

The structure of Equation 49 is such that it predicts (especially at high undercoolings, where non-steady-state effects are in general most significant, [46]) a shift of the $\log \tau^{\#}$ versus $1/T$ curves in a way similar to the already discussed shift of the $\log \eta$ versus $1/T$ curves for different pressures. An experimental confirmation of this behaviour is provided by the measurements of Mohan and Singh [47] on the kinetics of nucleation in Se-melts under pressure (Fig. 14).

A comparison with Fig. 5 (although for a somewhat different temperature range) shows a parallelism between the shift of the induction periods and the viscosity of Se-melts as required by the derivations given in Section 5.

The effect of pressure on the overall crystallization kinetics follows directly from Equation 59 and from the above considerations for the $I_{SS}(P)$ and $g(P)$ dependences. Considering Equations 50 and 56 it follows that:

$$\Delta W_2(T,P) = (3/16)\,\Delta W(T,P_o)\,[f_2(P)/f_3(P)]\,\Delta\mu(0)/d_0^2 \tag{73}$$

i.e., the barrier ΔW_2 for two-dimensional nucleation has much smaller value than that for three-dimensional nucleation, ΔW. Thus in Equation 59, the determining factors are $U(P,T)$ and $\Delta W(T,P)$, and the pressure shift of the $\log(t_c)$ curves should be

determined by an equation similar to Equation 45. The previously mentioned paper on the crystallization of Se-melts under pressure [47] gives experimental evidence in this respect.

Equations 70–72 could, with some reservations, also be applied to the case when $\Delta V < 0$. There it could be expected that $T_{max}(P)$ follows in an analogous way the decrease in $T_m(P)$. Up to now, however, no experimental evidence has been provided of this conjecture for melt crystallization of liquids like water and gallium under increased pressure.

6. Discussion

The influence of hydrostatic pressure on melt crystallization is analysed in detail in the present contribution employing the classical capillary model of the theory of nucleation.

(1) A simple formalism is used to determine the influence of the two major factors (change of driving force $\Delta\mu$ and of the specific interface energy σ) on the thermodynamic barrier. It is found, employing a simple thermodynamic model, that as a rule for one-component systems $(\partial\sigma/\partial p)_T < 0$ should be expected. Existing experimental evidence, cited in connection with the shift of T_{max} with pressure (cf. Figs 9 and 11, and Equation 70), seem to indicate that this is actually the case in systems where appropriate measurements have been performed (B_2O_3 and $Li_2O{\cdot}2SiO_2$). In this sense further and more accurate nucleation experiments could give additional information about the $\partial\sigma/\partial p$ dependence at the cluster/melt interface.

(2) For substances with normal dilatation upon crystallization ($\Delta V > 0$), the kinetic barrier of nucleation under increased pressures is increased and the thermodynamic barrier decreases. Thus a maximum in the $I_{SS}(P)|_T$ curve has to be expected and the actual nucleation catalysis effect (even at $\partial\sigma/\partial p < 0$) is restricted to definite regions of undercooling and at considerable ΔV values (cf. Equations 62, 63, 67 and 68). A dramatic increase in I_{SS} (and a decrease in $\tau^{\#}(P)$) should be expected only for $\Delta V/V_c$ values higher than 10%. In most other cases (i.e., at normal dilatations of 1–5%) only a shift of the $I_{SS}(P)$ versus $g(P)$ curve in accordance with $T_m(P)$ should be expected, the course of this shift being determined by the sign of $(\partial\sigma/\partial p)_T$.

(3) The effect of pressure on the non-steady-state nucleation time lag $\tau^{\#}$ is such that the log $\tau^{\#}$ versus P curves follow the $\log_\eta(P)$ curves. The experimental evidence in this respect, obtained by Mohan and Singh [47], provides also an additional proof of the non-steady-state character of induction periods in the overall crystallization of glassforming melts in the vicinity of τ_g (see [20, 24, 43]).

(4) The derivations concerning nucleation were made here in the framework of the classical capillary model. Its shortcomings are discussed in detail in reference [20] and possible alternative approaches are also mentioned there. However, it turns out (see [20, 48]) that at present these alternative theoretical models (e.g., the atomistic model of nucleation) offer little possibilities of exploiting and predicting the influence of varying conditions on the nucleation processes. Knowing the restrictions of the classical nucleation model it is also interesting to compare the general results obtained here with a derivation outside this model. A simple qualitative possibility in this respect is provided by the activated complex theory approach. According to this very general treatment (cf. [30, 49]), the frequency, ξ, of fluctuations is given by:

$$\xi = (kT/h)\exp[-\Delta\Phi^*/kT) \tag{74}$$

where

$$\Delta\Phi^* = \Delta U^* - T\Delta S^* + p\Delta V^*$$

is the free energy of activation associated with the transition into the state of the hypothetical activated complex determining the rate of the process. ΔU^*, ΔS^* and ΔV^*denote as usual the values of the corresponding energy, entropy and volume differences between activated and ground states, h is Planck's constant. Thus under pressure we should expect:

$$\xi = \text{const} \times \exp[(-\Delta U^*/kT) - p\Delta V)^*] \tag{75}$$

This approach can be used also to determine the frequency of formation of heterophase fluctuations (e.g., of crystalline nuclei in undercooled melts.) It is interesting to note that Equation 75 determines a dependence of ξ on P (i.e., also of I_{SS} on P) which can be obtained when the $[f_3(P)]^3/f_2^2(P)$ function in Equations 47 and 50 are expanded (for medium $(P - P_o)$ values) as truncated Taylor power series. In this case:

$$\{[f_3(P)]^3/[f_2(P)]^2\} \cong 1 - C_o\Delta V(P - P_o) \tag{76}$$

the sign of $C_o = \text{const}/\Delta W_o$ depending on the sign of $(\partial\sigma/\partial p)_T$, i.e., on K_o in Equation 23.

It is also to be accounted for that the thermodynamic analysis determining $T_m(P)$ is restricted here to a linear dependence (see Equations 4 and 5), i.e., according to Fig. 1 to pressures of about 0.1–0.5 GPa. This does not change in principle the expected results on the influence of increased pressure at higher pressures (say up to 1–10 GPa) but nevertheless for quantitative considerations (above 1 GPa) more accurate approximations for $T_m(P)$ are necessary.

(5) An interesting result of the present contribution seems to be the possible effect of increased pressure for liquids where crystallization proceeds under negative dilatation ($\Delta V < 0$). Fig. 7 shows that in this case there are two possibilities: at temperatures and pressures for which $d\eta/dp > 0$ and at $d\eta/dp < 0$. In the latter case the reverse situation to the one derived here for $\Delta V > 0$ is to be expected: the static pressure reduces the kinetic factor but increases the thermodynamic barrier of nucleation and crystal growth. At $d\eta/dp > 0$ and $\Delta V < 0$, a decrease in crystallization rates is to be expected for any $P > P_o$.

(6) Simple calculations are in agreement with the above formalism and show that for systems with positive, normal ΔV values (i.e., $\Delta V/V_c \approx$ 1–5% as it is e.g., in the model $Li_2O{\cdot}2SiO_2$ glass) practically no nucleation catalysis can be expected in the vicinity of T_g nor at any other temperature at which extrusion pressure

techniques are applicable. Hence, there must be another cause for the experimentally observed crystallization in extrusion pressure experiments. In Part II of the present investigation it is shown that the flow induced decrease of viscosity η due to shear thinning and not a reduction of ΔW in the classical sense of nucleation catalysis is responsible for the observed crystallization effects under these conditions.

Possible technical applications could be found only in the crystallization of such melts where considerable positive dilatations upon crystallization (up to 15–20%) are to be expected (as in Bi_2O_3, Aziz *et al.* [6]).

(7) Taking into account the structure of the respective dependences it turns out that under hydrostatic pressure the non-steady-state time lag $\tau^{\#}(P)$ always increases. The steady-state nucleation rate may increase or decrease depending on the $\Delta V/V_c$ value and on the sign of the $(\partial\sigma/\partial p)_T$ dependence. As a rule pressure shifts the nucleation and crystal growth process to higher temperatures, where lower viscosities are to be expected. This seems to be the major effect of hydrostatic pressure on melt crystallization.

Possible applications of the above considerations to geological processes (magma crystallization under static pressure) deserve particular consideration because of the possible extreme pressures that can be expected.

7. Conclusions

The possibilities of increased hydrostatic pressure, P, so as to act as a nucleation catalyst in melt crystallization are investigated. It has been shown that the effect can account for:

(i) the change of the thermodynamic driving force of melt crystallization under pressure;

(ii) the change in specific interface energy, σ, of the interface crystal/melt; in order to do this a thermodynamic model was employed and it was shown that for the melt/crystal interface, as a rule, $(d\sigma/dp)_T < 0$;

(iii) the dependence of kinetic factors (viscosity η) on pressure.

Existing experimental evidence seems to confirm the $(d\sigma/dp) < 0$ prediction.

Acknowledgements

The results of the present investigation have been obtained as part of an Innovation Programme funded by the Deutsche Forschungs Gemeinschaft (DFG), Bonn. We would like to express our gratitude to the DFG, who made this international cooperative programme possible.

References

1. G. TAMMANN, "Die Aggregatzustände" (Leopold Voss Verlag, Leipzig, 1922).
2. M. HASSELBLATT, *Z. Anorg. allg. Chemie* **119** (1921) 325.
3. *Idem*, *ibid.* **119** (1921) 353.
4. N. N. SIROTA, in "Crystallization and phase transformations", edited by N. N. Sirota (Bielorussian Academy of Science Publishers, Minsk, 1962) p. 38 (in Russian).
5. D. R. UHLMANN, J. F. HAYS and D. TURNBULL, *Phys. Chem. Glasses* **7** (1966) 159.
6. M. J. AZIZ, E. NYGREN, J. F. HAYS and D. TURNBULL, *J. Appl. Phys.* **57** (1985) 2233.
7. V. N. FILIPOVICH and D. D. DMITRIEV, *Fizika i Khimiya Stekla* **1** (1975) 41.
8. *Idem*, *ibid.* **1** (1975) 106.
9. I. N. STRANSKI, *Phys. Z. Sowjetunion* **10** (1936) 694.
10. B. R. DURSCHANG, G. CARL, C. RÜSSEL, K. MARCHETTI and E. ROEDER, *Glastech. Ber. Glass. Sci. Technol.* **67** (1994) 171.
11. B. R. DURSCHANG, G. CARL, K. MARCHETTI, E. ROEDER and C. RÜSSEL, in Proceedings of Advances in Fusion and Processing of Glass, Würzburg, 1995, edited by A. Shaeffer and L. D. Pye (Glast. Ber., Frankfurt 1995) p. 172.
12. E. ROEDER, *J. Non-Cryst. Solids* **5** (1971) 377.
13. *Idem*, *ibid.* **7** (1972) 203.
14. D. I. H. ATKINSON and P. W. McMILLAN, *J. Mater. Sci.* **11** (1976) 989.
15. A. J. PENNINGS, J. M. A. van der MARK and H. C. BOOJI, *Kolloid. Z. u. Z. f. Polymere* **236** (1970) 99.
16. I. GUTZOW, A. DOBREVA and J. SCHMELZER, *J. Mater. Sci.* **28** (1993) 890.
17. *Idem*, *ibid.* **28** (1993) 901.
18. W. KLEMENT Jr., L. H. COHEN and G. C. KENNEDY, *J. Phys. Chem. Solids* **27** (1966) 171.
19. I. GUTZOW, A. DOBREVA and D. PYE, *J. Non-Cryst. Solids* **180** (1995) 117.
20. I. GUTZOW and J. SCHMELZER, "The vitreous state: structure, thermodynamics, rheology and crystallization" (Springer Verlag, Berlin, 1995).
21. K. ONO and S. KORD, in "Handbuch der Physik", Vol. 19, edited by S. Flügge (Springer Verlag, Berlin, 1960).
22. A. J. RUSSANOV, "Phasengleichgewichte und Oberflächenerscheinungen" (Akademie Verlag, Berlin, 1978).
23. J. C. ERIKSSON, *Acta Chem. Scan.* **16** (1962) 2199.
24. I. GUTZOW, D. KASHCHIEV and I. AVRAMOV, *J. Non-Cryst. Solids* **73** (1985) 477.
25. A. DOBREVA and I. GUTZOW, *ibid.* **162** (1993) 1.
26. *Idem*, *ibid.* **162** (1993) 13.
27. O. K. RICE, *J. Chem. Phys.* **15** (1947) 333.
28. T. HILL, *J. Phys. Chem.* **56** (1952) 526.
29. N. GORSKI, *Z. Phys. Chem.* (*L*) **270** (1989) 817.
30. S. GLASSTONE, K. J. LAIDLER and H. EYRING, "The theory of rate processes" (Princeton Univ. Press, New York, 1941).
31. D. S. SANDITOV and G. M. BATENEV, "Physical properties of disordered structures" (Nauka, Novosibirsk, 1982) (in Russian).
32. B. MACEDO and T. A. LITOVITZ, *J. Chem. Phys.* **42** (1965) 245.
33. I. GUTZOW, I. AVRAMOV and K. KÄSTNER, *J. Non-Cryst. Solids* **123** (1990) 97.
34. J. R. PARTINGTON, "The properties of liquids" (Longmans, London, 1955).
35. I. AVRAMOV, *Phys. Stat. Solidi* (*a*) **120** (1990) 133.
36. L. L. SPERRY and J. D. MACKENZIE, *Phys. Chem. Glasses* **9** (1968) 91.
37. H. BORCHERS, H. HAUSEN, K.-H. HELLWEGE, K. SCHÄFER and E. SCHMITT: "Landoft–Börnstein: Gahlenwerte und Funktionen aus Physik, Chemie, Astronomie, Geophysik und Technik, II Band: Teil (5a): eigenshaften der materie in ihren Aggregatzuständen" (Springer Verlag, Berlin, 1969) pp. 128–492.
38. M. P. LECHNER, "D'Ans-lax; Taschenbuch für Chemiker und physiker, Band I: physikalisch-chemische daten" (Springer Verlag, Berlin, 1990) p. 623.
39. J. P. HIRTH and G. M. POUND, "Condensation and evaporation: nucleation and growth kinetics" (Pergamon Press, Oxford, 1963).
40. I. V. MARKOV, "Crystal growth for beginners" (World Sci. Publ., Singapore, 1995).
41. I. GUTZOW, *Contemporary Phys.* **21** (1980) 121.
42. *Idem*, *ibid.* **21** (1980) 243.

43. I. GUTZOW and D. KASHCHIEV, in "Advances in nucleation and crystallization in glasses", edited by L. L. Hench and S. W. Freiman (Amer. Ceram. Soc., Columbus, OH, 1971) p. 10.
44. Y. I. FRENKEL, "The kinetic theory of liquids" (Oxford Univ. Press, Oxford, 1946).
45. D. J. M. BURKHARD and N. V. RUSSELL, *J. Non-Cryst. Solids* **171** (1994) 236.
46. I. GUTZOW and A. DOBREVA, in "Nucleation and crystallization in glasses and liquids", edited by M. Weinberg (Amer. Ceram. Soc., Columbus, OH, 1992) p. 151.
47. M. MOHAN and A. K. SINGH, *Phil. Mag.* (*B*) **67** (1993) 705.
48. R. PASCOVA and I. GUTZOW, in Proceedings of Fundamentals of Glass Science and Technology, 2nd ESG Conference, Venice, 1993, Suppl. *Riv. Stat. Sperim. Vetro* **23** (1993) 443.
49. K. J. LEIDLER, "Reaction kinetics", Vol. II: reactions in solution" (Pergamon Press, London, 1963).

Received 28 May 1996
and accepted 26 February 1997